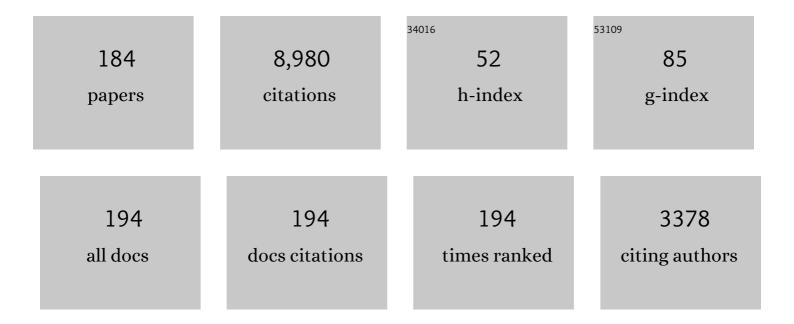
## Eduard Y Chekmenev

List of Publications by Year in descending order

Source: https://exaly.com/author-pdf/6580628/publications.pdf

Version: 2024-02-01



#	Article	IF	CITATIONS
1	Gas-Phase NMR of Hyperpolarized Propane with 1H-to-13C Polarization Transfer by PH-INEPT. Applied Magnetic Resonance, 2022, 53, 653-669.	0.6	6
2	Orderâ€Unity <sup>13</sup> C Nuclear Polarization of [1â€ <sup>13</sup> C]Pyruvate in Seconds and the Interplay of Water and SABRE Enhancement. ChemPhysChem, 2022, 23, .	1.0	30
3	Instrumentation for Hydrogenative Parahydrogen-Based Hyperpolarization Techniques. Analytical Chemistry, 2022, 94, 479-502.	3.2	52
4	Scanning Nuclear Spin Level Anticrossings by Constant-Adiabaticity Magnetic Field Sweeping of Parahydrogen-Induced <sup>13</sup> C Polarization. Journal of Physical Chemistry Letters, 2022, 13, 1925-1930.	2.1	8
5	Pilot Quality-Assurance Study of a Third-Generation Batch-Mode Clinical-Scale Automated Xenon-129 Hyperpolarizer. Molecules, 2022, 27, 1327.	1.7	3
6	Temperature Cycling Enables Efficient <sup>13</sup> C SABRE-SHEATH Hyperpolarization and Imaging of [1- <sup>13</sup> C]-Pyruvate. Journal of the American Chemical Society, 2022, 144, 282-287.	6.6	39
7	RASER MRI: Magnetic resonance images formed spontaneously exploiting cooperative nonlinear interaction. Science Advances, 2022, 8, .	4.7	12
8	<sup>15</sup> N NMR Hyperpolarization of Radiosensitizing Antibiotic Nimorazole by Reversible Parahydrogen Exchange in Microtesla Magnetic Fields. Angewandte Chemie, 2021, 133, 2436-2443.	1.6	6
9	<sup>15</sup> N NMR Hyperpolarization of Radiosensitizing Antibiotic Nimorazole by Reversible Parahydrogen Exchange in Microtesla Magnetic Fields. Angewandte Chemie - International Edition, 2021, 60, 2406-2413.	7.2	33
10	Lowâ€Flammable Parahydrogenâ€Polarized MRI Contrast Agents. Chemistry - A European Journal, 2021, 27, 2774-2781.	1.7	8
11	Heterogeneous Parahydrogenâ€Induced Polarization of Diethyl Ether for Magnetic Resonance Imaging Applications. Chemistry - A European Journal, 2021, 27, 1316-1322.	1.7	12
12	SABRE and PHIP pumped RASER and the route to chaos. Journal of Magnetic Resonance, 2021, 322, 106815.	1.2	19
13	Frontispiece: Heterogeneous Parahydrogenâ€Induced Polarization of Diethyl Ether for Magnetic Resonance Imaging Applications. Chemistry - A European Journal, 2021, 27, .	1.7	0
14	High field <i>para</i> hydrogen induced polarization of succinate and phospholactate. Physical Chemistry Chemical Physics, 2021, 23, 2320-2330.	1.3	8
15	Automated Low-Cost In Situ IR and NMR Spectroscopy Characterization of Clinical-Scale 129Xe Spin-Exchange Optical Pumping. Analytical Chemistry, 2021, 93, 3883-3888.	3.2	3
16	Clinical-Scale Production of Nearly Pure (>98.5%) Parahydrogen and Quantification by Benchtop NMR Spectroscopy. Analytical Chemistry, 2021, 93, 3594-3601.	3.2	27
17	PHIP hyperpolarized [1-13C]pyruvate and [1-13C]acetate esters via PH-INEPT polarization transfer monitored by 13C NMR and MRI. Scientific Reports, 2021, 11, 5646.	1.6	19
18	Synthesis and 15 N NMR Signal Amplification by Reversible Exchange of [ 15 N]Dalfampridine at Microtesla Magnetic Fields. ChemPhysChem, 2021, 22, 960-967.	1.0	8

#	Article	IF	CITATIONS
19	Bridging the Gap: From Homogeneous to Heterogeneous Parahydrogenâ€induced Hyperpolarization and Beyond. ChemPhysChem, 2021, 22, 710-715.	1.0	3
20	Synthetic Approaches for <sup>15</sup> N‣abeled Hyperpolarized Heterocyclic Molecular Imaging Agents for <sup>15</sup> N NMR Signal Amplification by Reversible Exchange in Microtesla Magnetic Fields. Chemistry - A European Journal, 2021, 27, 9727-9736.	1.7	9
21	Magnetic shielding of parahydrogen hyperpolarization experiments for the masses. Magnetic Resonance in Chemistry, 2021, 59, 1180-1186.	1.1	13
22	Heterogeneous <sup>1</sup> H and <sup>13</sup> C Parahydrogenâ€Induced Polarization of Acetate and Pyruvate Esters. ChemPhysChem, 2021, 22, 1389-1396.	1.0	9
23	Enabling Clinical Technologies for Hyperpolarized <sup>129</sup> Xenon Magnetic Resonance Imaging and Spectroscopy. Angewandte Chemie, 2021, 133, 22298-22319.	1.6	3
24	Low-Cost High-Pressure Clinical-Scale 50% Parahydrogen Generator Using Liquid Nitrogen at 77 K. Analytical Chemistry, 2021, 93, 8476-8483.	3.2	20
25	Enabling Clinical Technologies for Hyperpolarized <sup>129</sup> Xenon Magnetic Resonance Imaging and Spectroscopy. Angewandte Chemie - International Edition, 2021, 60, 22126-22147.	7.2	26
26	Hyperpolarization of common antifungal agents with SABRE. Magnetic Resonance in Chemistry, 2021, 59, 1225-1235.	1.1	8
27	Frontispiece: Synthetic Approaches for <sup>15</sup> Nâ€Labeled Hyperpolarized Heterocyclic Molecular Imaging Agents for <sup>15</sup> N NMR Signal Amplification by Reversible Exchange in Microtesla Magnetic Fields. Chemistry - A European Journal, 2021, 27, .	1.7	0
28	A Versatile Compact Parahydrogen Membrane Reactor. ChemPhysChem, 2021, 22, 2526-2534.	1.0	17
29	Backgroundâ€Free Proton NMR Spectroscopy with Radiofrequency Amplification by Stimulated Emission Radiation. Angewandte Chemie - International Edition, 2021, 60, 26298-26302.	7.2	12
30	Innentitelbild: Backgroundâ€Free Proton NMR Spectroscopy with Radiofrequency Amplification by Stimulated Emission Radiation (Angew. Chem. 50/2021). Angewandte Chemie, 2021, 133, 26206-26206.	1.6	0
31	New aspects of parahydrogen-induced polarization for C2—C3 hydrocarbons using metal complexes. Russian Chemical Bulletin, 2021, 70, 2382-2389.	0.4	4
32	"Direct― <sup>13</sup> C Hyperpolarization of <sup>13</sup> Câ€Acetate by MicroTesla NMR Signal Amplification by Reversible Exchange (SABRE). Angewandte Chemie - International Edition, 2020, 59, 418-423.	7.2	41
33	"Direct―13 C Hyperpolarization of 13 Câ€Acetate by MicroTesla NMR Signal Amplification by Reversible Exchange (SABRE). Angewandte Chemie, 2020, 132, 426-431.	1.6	16
34	Pulse-Programmable Magnetic Field Sweeping of Parahydrogen-Induced Polarization by Side Arm Hydrogenation. Analytical Chemistry, 2020, 92, 1340-1345.	3.2	28
35	XeUS: A second-generation automated open-source batch-mode clinical-scale hyperpolarizer. Journal of Magnetic Resonance, 2020, 319, 106813.	1.2	16
36	Quantifying the effects of quadrupolar sinks <i>via</i> <sup>15</sup> N relaxation dynamics in metronidazoles hyperpolarized <i>via</i> SABRE-SHEATH. Chemical Communications, 2020, 56, 9098-9101.	2.2	32

#	Article	IF	CITATIONS
37	Parahydrogenâ€Induced Polarization of Diethyl Ether Anesthetic. Chemistry - A European Journal, 2020, 26, 13621-13626.	1.7	11
38	Automated pneumatic shuttle for magnetic field cycling and parahydrogen hyperpolarized multidimensional NMR. Journal of Magnetic Resonance, 2020, 312, 106700.	1.2	16
39	High-Pressure Clinical-Scale 87% Parahydrogen Generator. Analytical Chemistry, 2020, 92, 15280-15284.	3.2	16
40	Frontispiece: Parahydrogenâ€Induced Polarization of Diethyl Ether Anesthetic. Chemistry - A European Journal, 2020, 26, .	1.7	0
41	Functional stability of water wire–carbonyl interactions in an ion channel. Proceedings of the National Academy of Sciences of the United States of America, 2020, 117, 11908-11915.	3.3	32
42	Pilot multi-site quality assurance study of batch-mode clinical-scale automated xenon-129 hyperpolarizers. Journal of Magnetic Resonance, 2020, 316, 106755.	1.2	9
43	Parahydrogen-Induced Magnetization of Jovian Planets?. ACS Earth and Space Chemistry, 2020, 4, 495-498.	1.2	3
44	Parahydrogenâ€Induced Radio Amplification by Stimulated Emission of Radiation. Angewandte Chemie - International Edition, 2020, 59, 8654-8660.	7.2	22
45	Parawasserstoffâ€induzierte Hyperpolarisation von Gasen. Angewandte Chemie, 2020, 132, 17940-17949.	1.6	1
46	Parahydrogenâ€Induced Radio Amplification by Stimulated Emission of Radiation. Angewandte Chemie, 2020, 132, 8732-8738.	1.6	14
47	Batch-Mode Clinical-Scale Optical Hyperpolarization of Xenon-129 Using an Aluminum Jacket with Rapid Temperature Ramping. Analytical Chemistry, 2020, 92, 4309-4316.	3.2	19
48	Parahydrogenâ€Induced Hyperpolarization of Gases. Angewandte Chemie - International Edition, 2020, 59, 17788-17797.	7.2	27
49	High Xe density, high photon flux, stopped-flow spin-exchange optical pumping: Simulations versus experiments. Journal of Magnetic Resonance, 2020, 312, 106686.	1.2	12
50	Helium-rich mixtures for improved batch-mode clinical-scale spin-exchange optical pumping of Xenon-129. Journal of Magnetic Resonance, 2020, 315, 106739.	1.2	6
51	Relayed nuclear Overhauser enhancement sensitivity to membrane Cho phospholipids. Magnetic Resonance in Medicine, 2020, 84, 1961-1976.	1.9	16
52	Cyclopropane Hydrogenation vs Isomerization over Pt and Pt–Sn Intermetallic Nanoparticle Catalysts: A Parahydrogen Spin-Labeling Study. Journal of Physical Chemistry C, 2020, 124, 8304-8309.	1.5	14
53	Rational ligand choice extends the SABRE substrate scope. Chemical Communications, 2020, 56, 9336-9339.	2.2	23
54	Quasi-Resonance Fluorine-19 Signal Amplification by Reversible Exchange. Journal of Physical Chemistry Letters, 2019, 10, 4229-4236.	2.1	23

#	Article	IF	CITATIONS
55	15 N Hyperpolarization of Dalfampridine at Natural Abundance for Magnetic Resonance Imaging. Chemistry - A European Journal, 2019, 25, 12694-12697.	1.7	18
56	NMR for Biological Systems. ChemPhysChem, 2019, 20, 177-177.	1.0	0
57	Unveiling coherentlyÂdriven hyperpolarization dynamics in signal amplification by reversible exchange. Nature Communications, 2019, 10, 395.	5.8	36
58	Parahydrogen-Induced Polarization of 1- <sup>13</sup> C-Acetates and 1- <sup>13</sup> C-Pyruvates Using Sidearm Hydrogenation of Vinyl, Allyl, and Propargyl Esters. Journal of Physical Chemistry C, 2019, 123, 12827-12840.	1.5	28
59	Clinical-Scale Batch-Mode Production of Hyperpolarized Propane Gas for MRI. Analytical Chemistry, 2019, 91, 4741-4746.	3.2	23
60	Hyperpolarizing Concentrated Metronidazole <sup>15</sup> NO <sub>2</sub> Group over Six Chemical Bonds with More than 15 % Polarization and a 20â€Minute Lifetime. Chemistry - A European Journal, 2019, 25, 8829-8836.	1.7	48
61	Relaxation Dynamics of Nuclear Long-Lived Spin States in Propane and Propane-d6 Hyperpolarized by Parahydrogen. Journal of Physical Chemistry C, 2019, 123, 11734-11744.	1.5	18
62	<sup>15</sup> N MRI of SLICâ€6ABRE Hyperpolarized <sup>15</sup> Nâ€Labelled Pyridine and Nicotinamide. Chemistry - A European Journal, 2019, 25, 8465-8470.	1.7	33
63	Limits of Spatial Resolution of Phase Encoding Dimensions in MRI of Metals. Journal of Physical Chemistry Letters, 2019, 10, 375-379.	2.1	1
64	Heterogeneous hydrogenation of phenylalkynes with parahydrogen: hyperpolarization, reaction selectivity, and kinetics. Physical Chemistry Chemical Physics, 2019, 21, 26477-26482.	1.3	12
65	A versatile synthetic route to the preparation of <sup>15</sup> N heterocycles. Journal of Labelled Compounds and Radiopharmaceuticals, 2019, 62, 892-902.	0.5	7
66	Unique Insights into the Structural and Functional Biology of Membrane Proteins from Solid State NMR Spectroscopy. Biophysical Journal, 2018, 114, 207a.	0.2	1
67	Parahydrogenâ€Based Hyperpolarization for Biomedicine. Angewandte Chemie - International Edition, 2018, 57, 11140-11162.	7.2	251
68	Spin–Lattice Relaxation of Hyperpolarized Metronidazole in Signal Amplification by Reversible Exchange in Micro-Tesla Fields. Journal of Physical Chemistry C, 2018, 122, 4984-4996.	1.5	45
69	Gramicidin Ion Binding and Conductance: New Insights from 17O Solid State NMR Spectroscopy in a 1.5 GHZ Spectrometer. Biophysical Journal, 2018, 114, 305a-306a.	0.2	0
70	Quasi-Resonance Signal Amplification by Reversible Exchange. Journal of Physical Chemistry Letters, 2018, 9, 6136-6142.	2.1	35
71	Effects of Deuteration of <sup>13</sup> C-Enriched Phospholactate on Efficiency of Parahydrogen-Induced Polarization by Magnetic Field Cycling. Journal of Physical Chemistry C, 2018, 122, 24740-24749.	1.5	12
72	Chemical Exchange Reaction Effect on Polarization Transfer Efficiency in SLIC-SABRE. Journal of Physical Chemistry A, 2018, 122, 9107-9114.	1.1	33

#	Article	IF	CITATIONS
73	<sup>19</sup> F Hyperpolarization of <sup>15</sup> N-3- <sup>19</sup> F-Pyridine via Signal Amplification by Reversible Exchange. Journal of Physical Chemistry C, 2018, 122, 23002-23010.	1.5	23
74	Hyperpolarized NMR Spectroscopy: <i>d</i> â€DNP, PHIP, and SABRE Techniques. Chemistry - an Asian Journal, 2018, 13, 1857-1871.	1.7	180
75	Facile Removal of Homogeneous SABRE Catalysts for Purifying Hyperpolarized Metronidazole, a Potential Hypoxia Sensor. Journal of Physical Chemistry C, 2018, 122, 16848-16852.	1.5	69
76	Synthesis of Unsaturated Precursors for Parahydrogen-Induced Polarization and Molecular Imaging of 1- <sup>13</sup> C-Acetates and 1- <sup>13</sup> C-Pyruvates via Side Arm Hydrogenation. ACS Omega, 2018, 3, 6673-6682.	1.6	33
77	Heterogeneous Parahydrogen Pairwise Addition to Cyclopropane. ChemPhysChem, 2018, 19, 2621-2626.	1.0	19
78	Parawasserstoffâ€basierte Hyperpolarisierung für die Biomedizin. Angewandte Chemie, 2018, 130, 11310-11333.	1.6	54
79	NMR Spectroscopy Techniques: Hyperpolarization for Sensitivity Enhancement. , 2018, , 168-168.		1
80	Toward Cleavable Metabolic/pH Sensing "Double Agents―Hyperpolarized by NMR Signal Amplification by Reversible Exchange. Chemistry - A European Journal, 2018, 24, 10641-10645.	1.7	13
81	NMR Hyperpolarization Techniques of Gases. Chemistry - A European Journal, 2017, 23, 724-724.	1.7	1
82	NMR Spin-Lock Induced Crossing (SLIC) dispersion and long-lived spin states of gaseous propane at low magnetic field (0.05 T). Journal of Magnetic Resonance, 2017, 276, 78-85.	1.2	36
83	Generalizing, Extending, and Maximizing Nitrogen-15 Hyperpolarization Induced by Parahydrogen in Reversible Exchange. Journal of Physical Chemistry C, 2017, 121, 6626-6634.	1.5	112
84	Extending the Lifetime of Hyperpolarized Propane Gas through Reversible Dissolution. Journal of Physical Chemistry C, 2017, 121, 4481-4487.	1.5	18
85	2D Mapping of NMR Signal Enhancement and Relaxation for Heterogeneously Hyperpolarized Propane Gas. Journal of Physical Chemistry C, 2017, 121, 10038-10046.	1.5	31
86	Frontispiece: NMR Hyperpolarization Techniques of Gases. Chemistry - A European Journal, 2017, 23, .	1.7	2
87	Direct Hyperpolarization of Nitrogen-15 in Aqueous Media with Parahydrogen in Reversible Exchange. Journal of the American Chemical Society, 2017, 139, 7761-7767.	6.6	80
88	High-resolution hyperpolarized in vivo metabolic 13C spectroscopy at low magnetic field (48.7 mT) following murine tail-vein injection. Journal of Magnetic Resonance, 2017, 281, 246-252.	1.2	26
89	The Absence of Quadrupolar Nuclei Facilitates Efficient <sup>13</sup> C Hyperpolarization via Reversible Exchange with Parahydrogen. ChemPhysChem, 2017, 18, 1493-1498.	1.0	87
90	Heterogeneous Microtesla SABRE Enhancement of <sup>15</sup> N NMR Signals. Angewandte Chemie - International Edition, 2017, 56, 10433-10437.	7.2	58

#	Article	IF	CITATIONS
91	Toward Hyperpolarized <sup>19</sup> F Molecular Imaging via Reversible Exchange with Parahydrogen. ChemPhysChem, 2017, 18, 1961-1965.	1.0	57
92	Robust Imidazoleâ€ <sup>15</sup> N <sub>2</sub> Synthesis for Highâ€Resolution Lowâ€Field (0.05 T) <sup>15</sup> NÂHyperpolarized NMR Spectroscopy. ChemistrySelect, 2017, 2, 4478-4483.	0.7	27
93	Long-Lived <sup>13</sup> C <sub>2</sub> Nuclear Spin States Hyperpolarized by Parahydrogen in Reversible Exchange at Microtesla Fields. Journal of Physical Chemistry Letters, 2017, 8, 3008-3014.	2.1	63
94	A pulse programmable parahydrogen polarizer using a tunable electromagnet and dual channel NMR spectrometer. Journal of Magnetic Resonance, 2017, 284, 115-124.	1.2	24
95	Imaging of Biomolecular NMR Signals Amplified by Reversible Exchange with Parahydrogen Inside an MRI Scanner. Journal of Physical Chemistry C, 2017, 121, 25994-25999.	1.5	25
96	Spin Relays Enable Efficient Long-Range Heteronuclear Signal Amplification by Reversible Exchange. Journal of Physical Chemistry C, 2017, 121, 28425-28434.	1.5	46
97	Heterogeneous Microtesla SABRE Enhancement of <sup>15</sup> N NMR Signals. Angewandte Chemie, 2017, 129, 10569-10573.	1.6	27
98	Aqueous, Heterogeneous <i>para</i> -Hydrogen-Induced <sup>15</sup> N Polarization. Journal of Physical Chemistry C, 2017, 121, 15304-15309.	1.5	40
99	NMR Hyperpolarization Techniques of Gases. Chemistry - A European Journal, 2017, 23, 725-751.	1.7	140
100	<sup>15</sup> N Hyperpolarization of Imidazole- <sup>15</sup> N <sub>2</sub> for Magnetic Resonance pH Sensing via SABRE-SHEATH. ACS Sensors, 2016, 1, 640-644.	4.0	111
101	Production of Pure Aqueous <sup>13</sup> Câ€Hyperpolarized Acetate by Heterogeneous Parahydrogenâ€Induced Polarization. Chemistry - A European Journal, 2016, 22, 16446-16449.	1.7	36
102	Open-Source Automated Parahydrogen Hyperpolarizer for Molecular Imaging Using <sup>13</sup> C Metabolic Contrast Agents. Analytical Chemistry, 2016, 88, 8279-8288.	3.2	84
103	NMR Signal Amplification by Reversible Exchange of Sulfurâ€Heterocyclic Compounds Found In Petroleum. ChemistrySelect, 2016, 1, 2552-2555.	0.7	34
104	Efficient Batchâ€Mode Parahydrogenâ€Induced Polarization of Propane. ChemPhysChem, 2016, 17, 3395-3398.	1.0	13
105	Toward production of pure <sup>13</sup> C hyperpolarized metabolites using heterogeneous parahydrogen-induced polarization of ethyl[1- <sup>13</sup> C]acetate. RSC Advances, 2016, 6, 69728-69732.	1.7	28
106	NMR SLIC Sensing of Hydrogenation Reactions Using Parahydrogen in Low Magnetic Fields. Journal of Physical Chemistry C, 2016, 120, 29098-29106.	1.5	21
107	Direct and cost-efficient hyperpolarization of long-lived nuclear spin states on universal <sup>15</sup> N <sub>2</sub> -diazirine molecular tags. Science Advances, 2016, 2, e1501438.	4.7	193
108	Efficient Synthesis of Molecular Precursors for Paraâ€Hydrogenâ€Induced Polarization of Ethyl	79	53

Acetateâ€lâ€< sup>13</sup>C and Beyond. Angewandte Chemie - International Edition, 2016, 55, 6071-6074.

#	Article	IF	CITATIONS
109	Over 20% <sup>15</sup> N Hyperpolarization in Under One Minute for Metronidazole, an Antibiotic and Hypoxia Probe. Journal of the American Chemical Society, 2016, 138, 8080-8083.	6.6	123
110	Aqueous NMR Signal Enhancement by Reversible Exchange in a Single Step Using Water-Soluble Catalysts. Journal of Physical Chemistry C, 2016, 120, 12149-12156.	1.5	63
111	Efficient Synthesis of Molecular Precursors for Paraâ€Hydrogenâ€Induced Polarization of Ethyl Acetateâ€1â€ <sup>13</sup> C and Beyond. Angewandte Chemie, 2016, 128, 6175-6178.	1.6	18
112	Efficient Synthesis of Nicotinamide-1- <sup>15</sup> N for Ultrafast NMR Hyperpolarization Using Parahydrogen. Bioconjugate Chemistry, 2016, 27, 878-882.	1.8	62
113	MR Imaging Biomarkers in Oncology Clinical Trials. Magnetic Resonance Imaging Clinics of North America, 2016, 24, 11-29.	0.6	33
114	Gas Phase UTE MRI of Propane and Propene. Tomography, 2016, 2, 49-55.	0.8	21
115	Microtesla SABRE Enables 10% Nitrogen-15 Nuclear Spin Polarization. Journal of the American Chemical Society, 2015, 137, 1404-1407.	6.6	275
116	NMR Hyperpolarization Techniques for Biomedicine. Chemistry - A European Journal, 2015, 21, 3156-3166.	1.7	247
117	Nanoscale Catalysts for NMR Signal Enhancement by Reversible Exchange. Journal of Physical Chemistry C, 2015, 119, 7525-7533.	1.5	61
118	Noninvasive Measurements of Glycogen in Perfused Mouse Livers Using Chemical Exchange Saturation Transfer NMR and Comparison to <sup>13</sup> C NMR Spectroscopy. Analytical Chemistry, 2015, 87, 5824-5830.	3.2	15
119	Hyperpolarization of "Neat―Liquids by NMR Signal Amplification by Reversible Exchange. Journal of Physical Chemistry Letters, 2015, 6, 1961-1967.	2.1	85
120	<sup>15</sup> N Hyperpolarization by Reversible Exchange Using SABRE-SHEATH. Journal of Physical Chemistry C, 2015, 119, 8786-8797.	1.5	192
121	Inhalable Curcumin: Offering the Potential for Translation to Imaging and Treatment of Alzheimer's Disease. Journal of Alzheimer's Disease, 2015, 44, 283-295.	1.2	40
122	Propane- <i>d</i> <sub>6</sub> Heterogeneously Hyperpolarized by Parahydrogen. Journal of Physical Chemistry C, 2014, 118, 28234-28243.	1.5	71
123	Dephosphorylation and biodistribution of 1â€ <sup>13</sup> Câ€phospholactate <i>in vivo</i> . Journal of Labelled Compounds and Radiopharmaceuticals, 2014, 57, 517-524.	0.5	26
124	Imaging amide proton transfer and nuclear overhauser enhancement using chemical exchange rotation transfer (CERT). Magnetic Resonance in Medicine, 2014, 72, 471-476.	1.9	62
125	Subâ€second proton imaging of <sup>13</sup> C hyperpolarized contrast agents in water. Contrast Media and Molecular Imaging, 2014, 9, 333-341.	0.4	22
126	The Feasibility of Formation and Kinetics of NMR Signal Amplification by Reversible Exchange (SABRE) at High Magnetic Field (9.4 T). Journal of the American Chemical Society, 2014, 136, 3322-3325.	6.6	148

#	Article	IF	CITATIONS
127	A 3D-Printed High Power Nuclear Spin Polarizer. Journal of the American Chemical Society, 2014, 136, 1636-1642.	6.6	72
128	High-Resolution Structures and Orientations of Antimicrobial Peptides Piscidin 1 and Piscidin 3 in Fluid Bilayers Reveal Tilting, Kinking, and Bilayer Immersion. Journal of the American Chemical Society, 2014, 136, 3491-3504.	6.6	78
129	Irreversible Catalyst Activation Enables Hyperpolarization and Water Solubility for NMR Signal Amplification by Reversible Exchange. Journal of Physical Chemistry B, 2014, 118, 13882-13889.	1.2	131
130	In Situ and Ex Situ Lowâ€Field NMR Spectroscopy and MRI Endowed by SABRE Hyperpolarization. ChemPhysChem, 2014, 15, 4100-4107.	1.0	58
131	Multidimensional Mapping of Spin-Exchange Optical Pumping in Clinical-Scale Batch-Mode 129Xe Hyperpolarizers. Journal of Physical Chemistry B, 2014, 118, 4809-4816.	1.2	32
132	Sodium 3D COncentration MApping (COMA 3D) using 23Na and proton MRI. Journal of Magnetic Resonance, 2014, 247, 88-95.	1.2	0
133	Temperature-Ramped <sup>129</sup> Xe Spin-Exchange Optical Pumping. Analytical Chemistry, 2014, 86, 8206-8212.	3.2	37
134	LIGHT-SABRE enables efficient in-magnet catalytic hyperpolarization. Journal of Magnetic Resonance, 2014, 248, 23-26.	1.2	151
135	Parahydrogen Induced Polarization of 1- <sup>13</sup> C-Phospholactate- <i>d</i> <sub>2</sub> for Biomedical Imaging with >30,000,000-fold NMR Signal Enhancement in Water. Analytical Chemistry, 2014, 86, 5601-5605.	3.2	83
136	Longâ€Lived Spin States for Lowâ€Field Hyperpolarized Gas MRI. Chemistry - A European Journal, 2014, 20, 14629-14632.	1.7	65
137	High-Resolution Low-Field Molecular Magnetic Resonance Imaging of Hyperpolarized Liquids. Analytical Chemistry, 2014, 86, 9042-9049.	3.2	39
138	Highâ€Resolution 3D Proton MRI of Hyperpolarized Gas Enabled by Parahydrogen and Rh/TiO <sub>2</sub> Heterogeneous Catalyst. Chemistry - A European Journal, 2014, 20, 11597-11597.	1.7	1
139	Toward hyperpolarized molecular imaging of HIV: synthesis and longitudinal relaxation properties of <sup>15</sup> Nâ€Azidothymidine. Journal of Labelled Compounds and Radiopharmaceuticals, 2014, 57, 621-624.	0.5	9
140	Heterogeneous Solution NMR Signal Amplification by Reversible Exchange. Angewandte Chemie - International Edition, 2014, 53, 7495-7498.	7.2	90
141	XeNA: An automated â€~open-source' 129Xe hyperpolarizer for clinical use. Magnetic Resonance Imaging, 2014, 32, 541-550.	1.0	57
142	Highâ€Resolution 3D Proton MRI of Hyperpolarized Gas Enabled by Parahydrogen and Rh/TiO <sub>2</sub> Heterogeneous Catalyst. Chemistry - A European Journal, 2014, 20, 11636-11639.	1.7	72
143	Demonstration of Heterogeneous Parahydrogen Induced Polarization Using Hyperpolarized Agent Migration from Dissolved Rh(I) Complex to Gas Phase. Analytical Chemistry, 2014, 86, 6192-6196.	3.2	27
144	Low-field MRI can be more sensitive than high-field MRI. Journal of Magnetic Resonance, 2013, 237, 169-174.	1.2	103

#	Article	IF	CITATIONS
145	Efficient Transformation of Parahydrogen Spin Order into Heteronuclear Magnetization. Journal of Physical Chemistry B, 2013, 117, 1219-1224.	1.2	51
146	Near-unity nuclear polarization with an open-source <sup>129</sup> Xe hyperpolarizer for NMR and MRI. Proceedings of the National Academy of Sciences of the United States of America, 2013, 110, 14150-14155.	3.3	193
147	Synthetic approach for unsaturated precursors for parahydrogen induced polarization of choline and its analogs. Journal of Labelled Compounds and Radiopharmaceuticals, 2013, 56, 655-662.	0.5	9
148	Current and emerging quantitative magnetic resonance imaging methods for assessing and predicting the response of breast cancer to neoadjuvant therapy. Breast Cancer: Targets and Therapy, 2012, 2012, 139.	1.0	20
149	A large volume double channel 1H–X RF probe for hyperpolarized magnetic resonance at 0.0475T. Journal of Magnetic Resonance, 2012, 220, 94-101.	1.2	27
150	PASADENA Hyperpolarized <sup>13</sup> C Phospholactate. Journal of the American Chemical Society, 2012, 134, 3957-3960.	6.6	70
151	Parahydrogen-Induced Polarization with a Rh-Based Monodentate Ligand in Water. Journal of Physical Chemistry Letters, 2012, 3, 3281-3285.	2.1	25
152	A pulsed injection parahydrogen generator and techniques for quantifying enrichment. Journal of Magnetic Resonance, 2012, 214, 258-262.	1.2	95
153	<i>In Situ</i> Detection of PHIP at 48 mT: Demonstration Using a Centrally Controlled Polarizer. Journal of the American Chemical Society, 2011, 133, 97-101.	6.6	75
154	Analysis of Cancer Metabolism by Imaging Hyperpolarized Nuclei: Prospects for Translation to Clinical Research. Neoplasia, 2011, 13, 81-97.	2.3	623
155	Parahydrogenâ€induced polarization (PHIP) hyperpolarized MR receptor imaging <i>in vivo</i> : a pilot study of <sup>13</sup> C imaging of atheroma in mice. NMR in Biomedicine, 2011, 24, 1023-1028.	1.6	116
156	Sodium MRI in a rat migraine model and a NEURON simulation study support a role for sodium in migraine. Cephalalgia, 2011, 31, 1254-1265.	1.8	34
157	Can antimicrobial peptides scavenge around a cell in less than a second?. Biochimica Et Biophysica Acta - Biomembranes, 2010, 1798, 228-234.	1.4	21
158	Toward C13 hyperpolarized biomarkers produced by thermal mixing with hyperpolarized X129e. Journal of Chemical Physics, 2009, 131, 044508.	1.2	10
159	Quality assurance of PASADENA hyperpolarization for 13C biomolecules. Magnetic Resonance Materials in Physics, Biology, and Medicine, 2009, 22, 123-134.	1.1	79
160	PASADENA hyperpolarization of 13C biomolecules: equipment design and installation. Magnetic Resonance Materials in Physics, Biology, and Medicine, 2009, 22, 111-121.	1.1	123
161	Hyperpolarized <sup>1</sup> H NMR Employing Low γ Nucleus for Spin Polarization Storage. Journal of the American Chemical Society, 2009, 131, 3164-3165.	6.6	77
162	Anisotropie Chemical Shift Perturbation Induced by Ions in Conducting Channels. , 2008, , 279-283.		0

#	Article	IF	CITATIONS
163	PASADENA Hyperpolarization of Succinic Acid for MRI and NMR Spectroscopy. Journal of the American Chemical Society, 2008, 130, 4212-4213.	6.6	170
164	Fluorine-19 NMR Chemical Shift Probes Molecular Binding to Lipid Membranes. Journal of Physical Chemistry B, 2008, 112, 6285-6287.	1.2	27
165	Towards hyperpolarized 13C-succinate imaging of brain cancer. Journal of Magnetic Resonance, 2007, 186, 150-155.	1.2	203
166	Low-E probe for 19F–1H NMR of dilute biological solids. Journal of Magnetic Resonance, 2007, 189, 182-189.	1.2	39
167	Using low-E resonators to reduce RF heating in biological samples for static solid-state NMR up to 900MHz. Journal of Magnetic Resonance, 2007, 185, 77-93.	1.2	172
168	High-Field NMR Studies of Molecular Recognition and Structureâ^'Function Relationships in Antimicrobial Piscidins at the Waterâ^'Lipid Bilayer Interface. Journal of the American Chemical Society, 2006, 128, 5308-5309.	6.6	39
169	Flow-Through Lipid Nanotube Arrays for Structure-Function Studies of Membrane Proteins by Solid-State NMR Spectroscopy. Biophysical Journal, 2006, 91, 3076-3084.	0.2	36
170	Ion-Binding Study by17O Solid-State NMR Spectroscopy in the Model Peptide Gly-Gly-Gly at 19.6 T. Journal of the American Chemical Society, 2006, 128, 9849-9855.	6.6	53
171	Peptide17O Chemical Shielding and Electric Field Gradient Tensors. Journal of Physical Chemistry B, 2006, 110, 22935-22941.	1.2	29
172	Two-Dimensional Solid-State NMR Reveals Two Topologies of Sarcolipin in Oriented Lipid Bilayersâ€. Biochemistry, 2006, 45, 10939-10946.	1.2	48
173	Investigating molecular recognition and biological function at interfaces using piscidins, antimicrobial peptides from fish. Biochimica Et Biophysica Acta - Biomembranes, 2006, 1758, 1359-1372.	1.4	69
174	Analysis of RF heating and sample stability in aligned static solid-state NMR spectroscopy. Journal of Magnetic Resonance, 2006, 180, 51-57.	1.2	33
175	A large volume flat coil probe for oriented membrane proteins. Journal of Magnetic Resonance, 2006, 181, 9-20.	1.2	33
176	15N and 31P solid-state NMR study of transmembrane domain alignment of M2 protein of influenza A virus in hydrated cylindrical lipid bilayers confined to anodic aluminum oxide nanopores. Journal of Magnetic Resonance, 2005, 173, 322-327.	1.2	32
177	Single-Crystal Studies of Peptide Prolyl and Glycyl15N Shielding Tensors. Journal of the American Chemical Society, 2005, 127, 9030-9035.	6.6	34
178	Ion Solvation by Channel Carbonyls Characterized by 17O Solid-State NMR at 21 T. Journal of the American Chemical Society, 2005, 127, 11922-11923.	6.6	56
179	Quantitative Observation of Backbone Disorder in Native Elastin. Journal of Biological Chemistry, 2004, 279, 7982-7987.	1.6	104
180	Synthesis and physico-chemical properties of peptides in soil humic substances. Chemical Biology and Drug Design, 2004, 63, 253-264.	1.2	20

#	Article	IF	CITATIONS
181	15N Chemical Shielding in Glycyl Tripeptides:Â Measurement by Solid-State NMR and Correlation with X-ray Structure. Journal of the American Chemical Society, 2004, 126, 379-384.	6.6	44
182	17O Quadrupole Coupling and Chemical Shielding Tensors in an H-bonded Carboxyl Group:  α-Oxalic Acid. Journal of the American Chemical Society, 2003, 125, 9140-9146.	6.6	33
183	Glycyl CαChemical Shielding in Tripeptides: Measurement by Solid-State NMR and Correlation with X-ray Structure and Theory. Journal of the American Chemical Society, 2002, 124, 11894-11899.	6.6	23
184	Backgroundâ€Free Proton NMR Spectroscopy with Radiofrequency Amplification by Stimulated Emission Radiation. Angewandte Chemie, 0, , .	1.6	2